# Traffic Hazards on Main Road's Bridges: Real-Time Estimating and Managing the Overload Risk

Roberto Ventura, Giulio Maternini, and Benedetto Barabino

*Abstract*— The risk associated with extreme traffic loads on bridges has seldom been explored, with State-of-the-art evaluation methods being time-consuming and unsuitable for fast risk management. Traditional risk management advocates optimizing offline bridge maintenance plans. In contrast, novel approaches that can assess and manage this risk live through Intelligent Transportation Systems (ITSs) are lacking. This study addresses these gaps with a three-block framework. It utilizes Weigh-In-Motion (WIM) systems for collecting bridge-specific traffic load data, develops a probabilistic Risk Prediction Model for estimating the frequency and severity of overloading events drawing on current Structural Design Codes (SDCs), and simulates an ITS-based architecture for implementing management actions. The framework was tested on 2.5M+ WIM raw data records gathered from the ring road of Brescia, Italy. Results showed that bridge design loads were overcome more frequently than SDCs prescriptions, and violations of the Traffic Code mass limit significantly affected risk predictions. These findings underscore the need for increased attention when issuing permits for extremely overweighted vehicles and encourage enforcement strategies implemented by ITS-based architectures for real-time risk management.

*Index Terms*— Bridge overload risk, bridge risk prediction models, weigh-in-motion, real-time bridge management strategies, traffic load hazard.

## I. INTRODUCTION

**B**RIDGES are among the most vulnerable elements of road networks because they may have structural issues that could compromise their use or, worst case, cause a collapse [1]. The whole transportation system is impacted by a bridge closure, being a negative event that lengthens user travel times, stops commodities from reaching their destinations and results in additional congestion [2]. After hydraulic actions, vehicular traffic is the primary element that affects bridge

safety. Indeed, a recent survey of more than 4,500 bridge failures worldwide from 2010 to 2016 revealed that overload and vehicle collisions are two of the top five most common reasons for failures [3].

Focusing on overload hazard, extremely heavy trucks are a threat for bridge safety. In fact, as traffic volume increases, truck loads routinely exceed bridge load limits, occasionally leading to collapses. These events are frequently observed in developed nations like the USA and Europe, as well as in developing ones like China (e.g., [3], [4], [5]).

Extremely heavy trucks can be subdivided into two categories: Permits (PMTs) and Illegally Overweighted Vehicles (IOVs) ( [6], [7], [8]). PMTs have a Gross Vehicular Mass (GVM) that exceeds the restrictions outlined in the Traffic Code (TC). However, they operate legally under permissions granted by Road Authorities (RA). Conversely, IOVs circulate without any permission and deserve attention as they elude the TC by travelling overweight.

Consequently, the implementation of Intelligent Transportation Systems (ITSs)-based architectures that integrate Weigh-In-Motion (WIM) devices for monitoring and managing the risk of extreme traffic loads is essential for ensuring bridge safety. WIM continuously measures vehicular attributes, including their masses (e.g., [9], [10], [11], [12]). These data could be processed to evaluate the risk of overloading on bridges. This would enable effective implementation of risk management measures, e.g., rerouting excessively heavy vehicles before reaching the bridge.

However, even if several methodologies for assessing and managing the risk of bridge failures have been described in the literature, the risk induced by extreme traffic loads has seldom been investigated. Research showed that: (i) the traffic load on bridges was almost exclusively obtained from literature models; (ii) the current risk metrics require time-consuming evaluation procedures, making a real time risk management strategy tricky; and (iii) ITS-based architectures, which safeguard bridges from overload by managing the traffic flows, are missing, as only optimization bridge maintenance plans that are conceived to operate offline are available. Given these scenarios, the objective of this study is to develop and test a three-block framework for estimating and managing the risk posed by extreme traffic load hazard. Specifically, the first block collects bridge-specific traffic load hazard data by WIM systems. The second block builds a time-dependent (bivariate) probabilistic Risk Prediction Model (RPM) by specifying, calibrating, and validating frequency and severity models, and accounting for the occurrences of overloading due to traffic

load hazard. The third block implements the RPM in an ITS-based architecture for achieving actual risk management.

The methodology was experimentally tested along the heavily transited ring road of the city of Brescia (Italy) using 2.5M+ WIM raw vehicular records gathered over five months by a pilot station located on an important bridge. The results can suggest methods for immediate risk evaluation and traffic management.

The remaining paper is organized as follows. Section II summarizes the literature on bridge failure risk analysis. Section III presents the framework for evaluating and managing extreme traffic load risk. Section IV shows a real-world experiment of the framework. Section V concludes the paper and provides future perspectives.

## II. LITERATURE REVIEW

### A. Methods of Bridge Risk Analysis

The risk of bridge failure was investigated in several ways. These typically differentiate between natural and anthropic hazards. The former are threats induced by natural events, such as floods, hurricanes, scour, tsunamis, and earthquakes (e.g., [13], [14]). The latter are menaces due to human activities, such as fires, blasts, terrorist attacks, vehicular collisions, and traffic loads (e.g., [15], [16]).

The risk induced by traffic loads is the focus of this research and has only been partially investigated in previous studies. The retrieved literature has been summarized in TABLE I, which illustrates the following main points.

The data adopted for risk analyses were gathered from different sources. Some countries (e.g., USA and UK) have public bridge databases (PBDs) along road networks. Consequently, these studies frequently collect data from PBDs. Conversely, other studies retrieved data from original design reports (ODR), on-site surveys (OSS), and, in some cases, by their integration with laboratory tests (LT). This is because these studies assess bridges located in other countries or require more detailed knowledge about structural parameters. The road network topology was gathered from open-source maps (OSM) or GIS databases. The traffic flow data along road links were directly collected by road agency archives, such as the FHWA Freight Analysis Framework tool (FAF) or computed by Origin-Destination matrixes (OD) provided by statistics institutes. Finally, while the traffic load on bridges was mainly obtained from models, only four papers analyzed field data collected by WIM devices.

The sample size was characterized by strong variability. Specifically, studies can be clustered for the number of investigated bridges. The first cluster included a few existing case-study bridges or fictitious bridges modeled by bridge design code specification. The second cluster was conceived at a network level, thus including studies ranging from small to very large bridge networks.

The literature provides contributions along three main directions according to the objective of the proposed analysis. The first direction is numerically predominant and assumes traffic load hazard as a component of a broader multi-hazard risk assessment framework (e.g., [17], [18], [19], [20]). For example, [17] proposed an approach for identifying, assessing, and quantifying risk on bridges resulting from numerous hazards, such as overload, fatigue, earthquake, storm surges, scour, vehicle collisions, and vessel collisions.

The second direction is numerically inferior and includes papers focused on traffic load hazards. For example, [2] and [21] proposed frameworks to quantify the risk on bridges along highway networks by considering vehicular overload effects and consequent fatigue phenomena. The number of trucks crossing the bridges, the percentage of these trucks that were overweight and the probability that overweight trucks could cross the bridge simultaneously were accounted for in the proposed models.

The third direction concerns only two studies assuming traffic load hazard as an input to merely estimate the consequences induced by bridge collapse. Specifically, [22] presented a detailed methodology to calculate the indirect losses accounting for the costs derived from the increase in traveled distance and travel time due to detours. Besides, [23] provided a broader insight of the possible consequences prompted by bridge failures considering repair costs (single element failures); rebuilding costs (entire system failure); traffic delay costs due to repair work and detours; traffic management costs during repair work; casualty costs involving vehicles falling from the bridge, vehicles hit by the fallen bridge, and vehicles crashing into the fallen bridge; and other indirect costs.

The modeling techniques primarily depend on the way in which the risk is intended: there is no agreement among researchers because at least two risk mathematical definitions emerge. The former definition states the risk as the sum of the probability of occurrence of each failure scenario times the associated (direct and indirect) consequences (e.g., [21], [24], [25]). The latter definition states the risk merely as the probability of occurrence of an undesired event (e.g., [26], [27]).

According to the first risk definition, tools were proposed for quantifying the two components. As for the probability of occurrence, the Reliability Analysis Method (RAM) was frequently adopted. It computes the reliability index, a parameter that is related to the failure probability, and that is a conventional tool for evaluating the safety of existing structures, according to current standards, such as Eurocodes. The reliability index was typically calculated using the structural performance function (SPF), as in [18], [20], [24], [28], and [29]. The SPF is defined as the difference between structural capacity and demand functions. It represents the structural failure condition when a negative value occurs. Specifically, the structural capacity function relied on geometrical and material properties. The structural demand function was often constructed by inferring the maximum traffic load on the bridge through extreme value theory.

It employed generalized extreme-value distributions, as observed in [18] and [28]. Occasionally, the RAM was integrated with fragility curves, describing the probability of failure as a function of hazard intensity ([2], [17], [21]). Fragility curves for the overload hazard were calculated using numerical simulations based on 3D non-linear grillage Finite Element Models (FEMs) of the

TABLE I
SUMMARY OF THE LITERATURE THAT ACCOUNTS FOR THE RISK INDUCED BY TRAFFIC LOADS ON BRIDGES

| Reference | Country | Data sources | Sample size[a] | Objective/Relevant insights | Modeling techniques |
|---|---|---|---|---|---|
| [2] | USA | WIM, PBD, FAF | 1,315 | Quantifying the importance of bridges along a highway network under overweight traffic loads and proposing a risk mitigation strategy. | TLM, RM, RAM, fragility curves, FEM, ETM, MCS, TNM |
| [17] | USA | WIM, PBD, USGS | 5,534 | Identifying and assessing risk on bridges resulting from different hazards. | RAM, fragility curves, CT |
| [18] | USA | L, OSS | 1 | Assessing time-variant risks associated with the closure of bridge lanes due to traffic loading and scour hazards. | TLM, TMD, SPF |
| [19] | USA | L, PBD | 5 | Assessing the life-cycle risk of aged bridges along a road network considering time-dependent vulnerability, earthquakes, and abnormal traffic hazards. | ETM, vulnerability analysis, RM, MCS |
| [20] | USA | PBD, USGS | 1 | Evaluating the time-dependent risk of highway bridges in a multi-hazard environment to rank the structures and prioritize interventions. | TLM, TMD, SPF, RAM |
| [21] | USA | WIM; PBD, FAF | 600 | Performing a life-cycle analysis of a bridge network exposed to vehicular overload and cyclic fatigue by minimizing the overall risk. | RAM, fragility curves, FEM, TLM, RM, ETM, LSNN |
| [22] | Italy | OSM, OD | 617 | Calculating indirect losses due to bridge collapses and evaluating the relative importance of bridges. | TNM |
| [23] | UK | PBD, L | 9 | Proposing a cost-evaluation method to assess the consequences induced by bridge failure to be applied in bridge-risk assessment. | Motion law analysis, impact speed/injury probability models, RM |
| [24] | USA | GTN | 10 | Optimizing life-cycle maintenance plans of bridge networks based on network-level risk minimization. | TLM, SPF, RAM, TNM, network-level risk bounds, GA |
| [26] | USA | PBD | 16,925 | Predicting the probability of a bridge being "at risk" according to the PBD condition score. | BLR |
| [27] | USA | SBF, PBD, EO | N/A | Analyzing the failure risk of segmental concrete box girder bridges. | FTA |
| [30] | China | WIM, TCAM, LI, A, SG, DG | N/A | Evaluating and predicting the working status of a group of bridges along a network through a digital twin system to implement a safety early warning system against overturning risk. | Cloud computing, machine vision fusion, FEM, MCS |
| [31] | USA | PBD, GIS, FHWA | 20 | Ranking bridges and suggesting maintenance priorities based on risk assessment. | RAM, MC, BU, TNM |
| [28] | USA | L, NBI | 1 | Developing a framework for life-cycle maintenance optimization of highway bridges based on network-level risk bounds. | TLM, TMD, SPF, RAM, GA |
| [32] | USA | PBD | 16 | Assessing the risk on bridge networks quantitatively under live loads and deterioration. | RAM, MC, TNM |
| [29] | N/A | L | 1(f) | Determining the optimal intervention for a bridge affected by traffic load and scour hazards. | TLM, TMD, SPF, RAM |
| [33] | USA | PBD, TS | 6,000 | Determining a bridge posting strategy that minimizes the risk on structures. | Decision flow chart |

[a] Number of analyzed bridges (f indicates that are fictious bridges).

**Acronym glossary:** A= Accelerometers; BLR = Binary Logistic Regression; BU = Bayesian Updating; B-WIM = Bridge Weight in Motion; CT = Classification Tree; DFC = Decision Flow Chart; DG = Displacement Gauges; EO = Expert Opinions; ETM = Event Tree Model; FAF = FHWA Freight Analysis Framework tool; FEM = Finite Elements Model; FTA = Fault-tree analysis; GA = Genetic Algorithm; GIS = Geographic Information System Database; GTN = Github Transportation Networks repository; ILM = Influence Line Method; L=Literature; LFT = Laboratory Fatigue Tests; LI = Lidar; LSNN = Local Search Nearest Neighbor Heuristic Algorithm; LT = Laboratory Tests; MC = Markov Chain; MCS = Monte Carlo Simulation; OD = Origin Destination Matrices; ODR= Original Design Reports; OSM = Open Source Map; OSS = On-Site Surveys; PBD = Public Bridges Database; RAM = Reliability Analysis Method; RM = Regression Model; SBF = Studies on Bridge Failures; SG = Strain Gauges; SPF = Structural Performance Function; TCAM = Traffic Cameras; TLM = Traffic Load Model based on previous literature; TMD = Time dependent material degradation model; TNM = Transportation Network Model; TS = Telephonic Surveys; USGS = United Stated Geological Survey database; WIM = Weight in Motion

bridge superstructures ([2], [21]) or through analytical formulations that considered the average daily truck traffic, the percentage of overweight trucks, and bridge deterioration ([17]), for example.

As for the associated consequences, direct failure consequences (e.g., rebuilding/repairing costs) were parametrically determined. Conversely, two approaches were employed regarding indirect consequences: (a) empirical and (b) analytical. For (a), the estimation of increased vehicular operating costs and users' travel time involved multiplying traffic volumes passing on the bridges and detour lengths by some parameters (e.g., average detour speed, average vehicular occupancies, marginal operating costs, marginal value of time). Additionally, costs related to injuries and fatalities were

estimated based on statistics computed from past bridge failure events (e.g., [17], [18], [28], [20]). Concerning (b), the computation of increased vehicular operating costs and users' travel time involved developing Transportation Network Models (TNMs) that simulated network damage states, as in [2], [22], [24], [31], and [32]. Similarly, costs associated with injuries and fatalities were determined using models that considered vehicular flows on the bridges, vehicular occupancy, safe following distance, impact speed/injury probability, and failure kinematics, as evidenced by [19], [23], and [34].

According to the second risk definition, [26] considered a binary response variable based on a PDB condition score and built a Binary Logistic Regression (BLR) model to predict it. Conversely, [27] defined the risk as the probability of collapse events and predicted them through a fault tree analysis (FTA). Finally, following the risk estimation, someone delved into identifying best maintenance actions to minimize the overall risk at the network level, employing optimization methods. For instance, [21] utilized a Local Search Nearest Neighbor Heuristic Algorithm (LSNN) to optimize the network's risk. This involved minimizing a cost function, expressed as the sum of costs associated with each individual bridge failure while adhering to a financial constraint imposed on the overall intervention cost. Additionally, in some cases, a Genetic Algorithm (GA) was utilized to determine the most suitable maintenance actions and the optimal timing for their implementation (e.g., [24], [28]).

### B. Literature Gaps and Proposed Advancements

Undoubtedly, all previous studies have contributed to the analysis of the risk induced by traffic load hazards on bridges with separate goals and provided valuable results. However, several gaps persist:

  i. The list of bridge-safety factors.
  ii. The source of analyzed data.
 iii. The computational effort required by current risk metrics.
 iv. The type of proposed risk management actions.

As for (i), no study has revealed, in single research, such a long list of the overall bridge safety factors, which may affect the frequency and the severity of bridge failures.

As for (ii), the traffic load acting on bridges was obtained from previously developed models in almost all studies. Indeed, although WIM systems are a well-known technology (e.g., [6]), only a few works analyzed field WIM raw data to propose a risk assessment and mitigation strategy based on maintenance plans. Nonetheless, because of traffic load hazard's strong spatial and temporal dependence, methods that assume actual bridge-specific data as input are essential to achieving an effective risk management strategy.

As for (iii), achieving a rapid computation of current risk metrics might be tricky for RAs. Indeed, existing methods require time-expensive elaborations for estimating the two risk components because: 1) refined structural analyses must be performed for evaluating the probability of occurrence of failure events by RAM, 2) refined cost and traffic analyses must be conducted for determining direct and indirect failure consequences. These sophisticated assessments could make it

difficult to implement an immediate risk management strategy, in which traffic management actions must be taken quickly to avoid bridge overload. Moreover, budget constraints often prevent RAs from calibrating such advanced structural, cost, and traffic models.

Nevertheless, a real-time risk management approach could outperform a static one. Therefore, a straightforward risk assessment procedure that accounts for the failure probability and consequences indirectly could add to existing procedures based on RAM, cost analysis, and traffic models. In fact, once the design traffic load thresholds have been determined according to the traffic load schemes outlined by the current Structural Design Codes (SDCs), a frequency and severity metric can be used that measures how often and how seriously these thresholds are exceeded in each time period. These metrics could serve as a catalyst for indirectly measuring the likelihood and the consequences of potential bridge failure occurrences prompted by traffic load hazard. Additionally, these metrics might be assessed using proper mathematical models that connect it to a set of predictors categorized into exposure, bridge side, temporal context, and traffic load hazard. These models, which mine from WIM datasets, could, thus, advance theoretical comprehension of the phenomena of bridge overload by understanding the impact of predictors on overload frequency and severity.

As for (iv), while many authors investigated the best bridge maintenance plans, only [33] provided a preliminary attempt to reduce traffic load-related risk by implementing a traffic management strategy. Nevertheless, they adopted a static procedure merely based on posting bridges for maximum allowable loads. In addition, although [30] developed a Digital Twin system to provide safety alerts against bridge overturning, no traffic management actions have been proposed. However, as bridge maintenance plans focus on bridge capacity rather than demand, traffic management measures implemented through ITS-based architectures could effectively reduce traffic load risk. Hence, ITS-based architectures that acquire site-traffic load data and act through immediate traffic management actions to reduce the risk of bridge overload should be investigated. This paper aims to cover all these gaps inclusively.

To summarize, the proposed framework significantly differs from the conventional methods (e.g., [2], [21]). Particularly, focusing on points (ii), (iii) and (iv), the main differences involve the following key aspects:

a. Indirectly measuring the probability of bridge failure events: while [2] and [21] directly employed the traditional RAM, this study introduces an innovative indirect approach. It assesses a frequency metric by counting traffic overloading events. Using an Econometric Model (EM), the frequency is straightforwardly linked to several traffic-related predictors derived from WIM records.[1]

---

[1]At the time of revising this paper, the authors were engaged in two other papers focused on comparing the performance of Econometric and Machine Learning models in predicting the frequency and severity metrics components separately (https://dx.doi.org/10.2139/ssrn.4417358 and https://doi.org/10.1016/j.heliyon.2023.e23374, respectively).
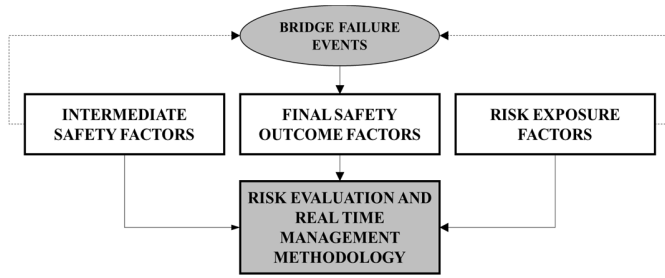
Fig. 1. Conceptual framework for bridge risk evaluation and real-time management.

b. Indirectly measuring the consequences of bridge failure events: while [2] and [21] directly evaluated cost metrics, this study introduces an innovative indirect method. It assesses a severity metric by categorizing traffic overloading events. Using an EM, the severity is straightforwardly linked to several traffic-related predictors derived from WIM records.[1]

c. Mitigating the risk of bridge failure events by traffic management actions: while [2] and [21] proposed static risk mitigation strategies, this study suggests a live approach. It introduces dynamic traffic management actions by ITS technologies like traffic lights, variable message signals, and cloud computing platforms to reroute high-risk vehicle platoons away from bridges.

## III. CONCEPTUAL FRAMEWORK FOR BRIDGE RISK EVALUATION AND REAL-TIME MANAGEMENT

The conceptual framework for bridge risk evaluation and management is described in this section. It defines the steps of a bridge failure event according to specific factors and integrates them into a risk assessment methodology while providing management strategies for its mitigation. *Fig. 1* provides a scheme of this framework, described in what follows.

### A. Conceptual Construction and Bridge Failure Factors

A bridge failure event is induced by the interaction of four groups of factors: bridge-side factors, context factors, anthropogenic hazard factors and natural hazards factors. In this research, all these factors are denoted as "***intermediate safety factors***," borrowing the well-accepted definitions suggested by ISO 39001 [35] for road safety analysis and adapting it to the scope of bridge risk assessment.

Further factors may be defined to measure the number of vehicles and individuals that could induce or be interested by bridge failure events. They are referred to as "***risk exposure factors***," according to ISO 39001 [35].

Consequently, the interaction between the intermediate safety and risk exposure factors leads to the occurrence of bridge failure events. Moreover, both factors may affect the probability (or the frequency) of bridge failure events and their severity. The frequency and severity of bridge failure events are reflected in several outcome factors. This study refers to them as "***final safety outcome factors***," according to ISO 39001 [35].

Drawing on the previous literature, Parts A, B and C reported in the Supplementary Material section provide a census of intermediate, risk exposure and final safety factors, respectively. They are organized in a multi-level hierarchy.

### B. Methodology for Real-Time Risk Evaluation and Management

The proposed framework is focused on the risk of overloading events induced by extreme traffic load hazard and is organized into three main blocks, each of which meets a specific requirement as follows:

- Block 1 operates "offline" to collect data on the traffic on the bridge and handles these data to obtain a bridge-specific traffic load hazard dataset.
- Block 2 operates "offline" to specify, calibrate, and validate a time-dependent (bivariate) Risk Prediction Model (RPM).
- Block 3 operates "online" to achieve live risk management by implementing an ITS-based architecture.

Each block is subdivided into several steps, described and formulated in the flowchart shown in Fig. 2. It is noteworthy that, to enable real-time risk management, the computational complexity of "online" processes must be short. Thus, this need is addressed by designing the most time-consuming computational processes in Block 1 and Block 2. They are intended "offline" before starting the risk management phase, which exclusively operates "online" in Block 3.

*1) BLOCK 1: Build a Bridge-Specific Traffic Load Hazard Dataset:* Block 1 is organized in 5 steps. According to Step 1.1, the first block starts with raw data traffic load collection during a monitoring period by WIM systems. They are placed on each lane of a road section near the bridge. For each passing vehicle, a standard WIM architecture measures the passing datetime, the gross vehicular mass, the passing speed, the vehicular length, the vehicular width, the number of axles, the typology of each axle (i.e., single or double wheel), the mass acting on each axle, and the distance between each pair of axles (i.e., interaxle).

From these measures, a dataset of raw bridge-specific experimental records is mined. More formally, let:

- $T$ be the monitoring period and $t \in T$ [s] the generic timestamp (or instant).
- $I$ be the set of bridge lanes and $i \in I$ be the generic lane.
- $VEH(T, i)$ be the set of vehicles recorded by WIM during $T$ along $i \in I$ and $veh \in VEH(T, i)$ be the generic vehicle.
- $U$ be the set of vehicular classes recognized by the WIM system and $u \in U$ be the generic class.
- $GVM(veh)$ [kg] be the Gross Vehicular Mass of $veh \in VEH(T, i)$, i.e., the total mass of the vehicle.
- $speed(veh)$ [km/h] be the passing speed of $veh \in VEH(T, i)$, i.e., the mean passing speed among all vehicular axles.
- $length(veh)$ [m] be the vehicular length of $veh \in VEH(T, i)$, i.e., the distance from the first and the last axles.
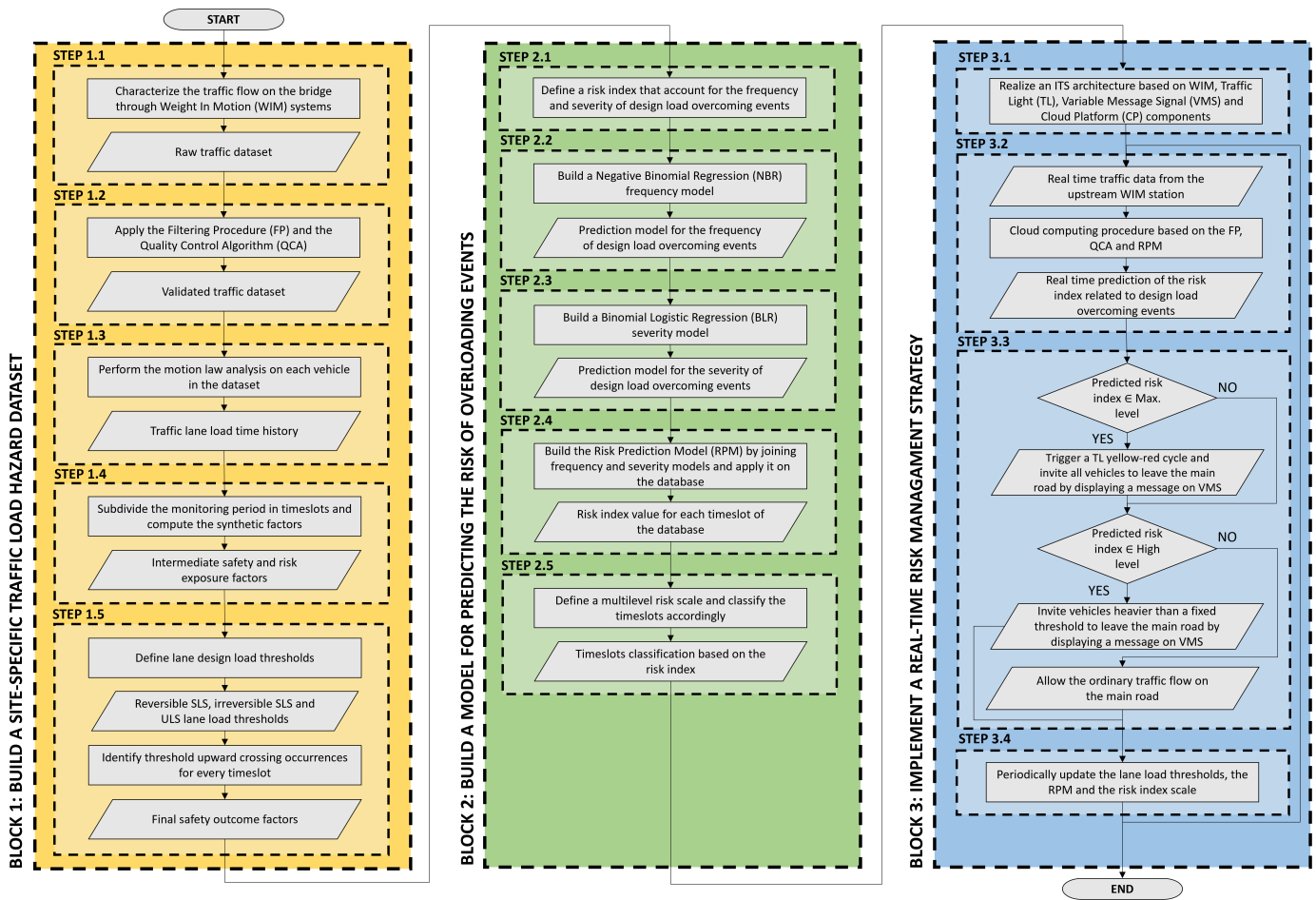
Fig. 2.   Methodology for the evaluation and real-time management of the risk induced by extreme traffic load hazard.

- $AXL(veh)$ be the set of axles of $veh \in VEH(T, i)$ and $axl_k \in AXL(veh)$ be the k-th axle.
- $type(axl_k)$ be the typology of $axl_k \in AXL(veh)$, which could be single wheel or double wheel.
- $mass(axl_k)$ [kg] be the mass acting on $axl_k \in AXL(veh)$.
- $INT(veh)$ be the set of interaxle of $veh \in VEH(T, i)$ and $int_r \in INT(veh)$ [m] be the r-th interaxle.

Next, according to Step 1.2, the WIM raw data undergo pre-processing to eliminate anomalies and outliers using a designated Filtering Procedure (FP) and Quality Control Algorithm (QCA), respectively. Following the application of FP and QCA, a validated traffic dataset is obtained. Additional information about the pre-processing methods can be found in PART D (Section I) of the Supplementary Material section.

Next, according to Step 1.3, for each bridge lane $i \in I$, the overall vehicular load acting on it in each instant $t \in T$ (denoted as $G_i(t)$ [$kN$]) is computed from the validated traffic dataset. Its determination is mandatory for the subsequent identification of overloading events induced by traffic. Since the bridge deck has a certain length, and the WIM system only provides records of axles at a single point, it is necessary to ascertain the law of motion of each axle (i.e., $axl_k \in AXL(veh)$; $\forall veh \in VEH(T, i)$) along $i \in I$. This enables the determination

of the application point of each load at times other than its passage on the WIM. The formalization of this procedure is presented in PART E of the Supplementary Material section.

Next, according to Step 1.4, the monitoring period (i.e., $T$) is further divided into temporal frames (or timeslots) to investigate how the characteristics of the vehicles passing on the bridge varies over the time. More formally, let $S$ be the set of timeslots and $T(s)$ be the subset of $T$ in the timeslot $s \in S$. Then intermediate safety and risk exposure factors of traffic load hazard are computed on the traffic flow observed during $T(s)$.

According to Step 1.5, the final safety outcome factors are computed to account for the frequency and severity of bridge failure events induced by traffic load hazard. Among these factors, those related to limit states are selected for two main reasons: 1) the Limit State Method (LSM) is widely adopted by current Structural Design Codes (SDCs), e.g., the Eurocodes and the Italian NTC ( [36], [37]), that are well known among researchers and practitioners; 2) limit states enable to account for the seriousness of bridge failure events in a faster way than direct and indirect consequence factors. According to the LSM, a "bridge failure" does not necessarily indicate a collapse; rather, it is defined as any situation (e.g., the overcoming of a "limit state") that could lead to a malfunction in the system.

| Load combination | Limit state for which the load combination is prescribed | Associated design traffic lane load threshold [kN] |
|---|---|---|
| Fundamental Combination (FuC) | Ultimate Limit State (ULS) | $th(FuC)_i$ |
| Characteristic Combination (ChC) | Irreversible Serviceability Limit State (ISLS) | $th(ChC)_i$ |
| Frequent Combination (FrC) | Reversible Serviceability Limit State (RSLS) | $th(FrC)_i$ |

In the proposed framework, the rigorous individuation of limit states overcoming events is replaced by a more straightforward detection of design lane load overcoming events, as budget constraints frequently prevent road management authorities from the calibration of a refined structural model. Hence, a set of different design traffic lane load thresholds is defined. These thresholds are related to different degrees of magnitude of the effects suffered by the bridge when they are exceeded.

More precisely, let $TH$ be the set of traffic lane design load thresholds and $th_i \in TH$ be the generic threshold for $i \in I$. The traffic load schemes proposed by current SDCs can be assumed as reference to a straightforward quantification of each $th_i \in TH$. For example, [36] and [37] prescribe various load combinations linked to varying levels of solicitation magnitudes These combinations are intended for use in verifying different limit states, as outlined in TABLE II. These load models rely on several considerations to achieve a target reliability level, including, for example, a 1,000-year return period of the characteristic value, a dynamic amplification factor (which depends on pavement roughness, roughness, and vehicle properties), and future increases in traffic.

Next, to obtain the input data for the risk model fitting, the count and typology of overloading events are determined for each timeslot $s \in S$ and lane $i \in I$. An overloading event is defined as a circumstance in which the traffic load on the lane $i \in I$ exceeds one or more design load thresholds. More formally, let:

- $DLO$ be the set of design load overcoming events and $dlo \in DLO$ the generic event.
- $DLO(th_i, s)$ be the subset of $DLO$ related to the overcoming events of $th_i \in TH$ during $T(s)$ on $i \in I$.

Therefore, for each $t \in T(s)$, $th_i \in TH$ and $i \in I$, the generic $dlo \in DLO(th_i, s)$ is identified when the load is lower or equal than the considered threshold (i.e., $G_i(t) \le th_i$) and, in the instant immediately after $t + dt \in T(s)$, the load is higher than the same threshold (i.e., $G_i(t + dt) > th_i$). More formally:

$$dlo \in DLO(th_i, s)$$
$$\Longleftrightarrow$$
$$(G_i(t) \le th_i) \,\&\, (G_i(t + dt) > th_i);$$
$$\forall th_i \in TH; \; \forall t \in T(s); \; \forall s \in S; \; \forall i \in I \qquad (1)$$

Thus, by computing each $DLO(th_i, s)$, the final safety outcome factors are obtained.

*2) BLOCK 2: Build a Model for Predicting the Risk of Overloading Events:* Block 2 is organized in 5 steps. According to Step 2.1, an index is defined to evaluate the risk connected to the design load overcoming events induced by the traffic hazard. There are some methods that may be applied to evaluate the risk. In this study, we considered a time-dependent index. It integrates frequency and severity functions of the design overloading events, as well as the exposure factors accounting for all the intermediate outcome factors considered. This choice is due to the possibility of specifying each function according to the WIM data and simplifying the interpretability of its outcomes among practitioners. The risk index is evaluated as follows. Let:

- $E_s$ be the exposure factor during $T(s)$, intended as the rate of occurrence of the hazard event (i.e., a traffic load application on the bridge).
- $P_s$ be the probability factor during $T(s)$, intended as the likelihood that, once the hazard event occurs, the complete loading sequence will follow with the necessary timing and coincidence to result in a design load overcoming event.
- $C_s$ be the consequences during $T(s)$, intended as the most probable result of a design load overcoming event, including direct and indirect costs.
- $H_s$ be the frequency of design load overcoming events during $T(s)$, intended as a driver of the probability of design load overcoming events.
- $V_s$ be the severity of design load overcoming events during $T(s)$, intended as a driver of the consequences of design load overcoming events.
- $X$ be the set of frequency predictors, $x_j \in X$ be the $j^{th}$ predictor and $x_{j,s}$ be the value of $x_j \in X$ observed in $T(s)$.
- $Y$ be the set of severity predictors, $y_j \in Y$ be the $j^{th}$ predictor and $y_{j,s}$ be the value of $y_j \in Y$ observed in $T(s)$.

According to the well-accepted concept of risk, the risk index related to $s \in S$ (denoted by $R_s$) may be defined as follows [38]:

$$R_s \stackrel{\text{def}}{=} E_s * P_s * C_s; \quad \forall \, s \in S \qquad (2)$$

Although the calculation of (2) is simple, each term needs to be estimated by modeling the experimental data. A way to perform this task is to build a complete bivariate risk model (frequency and severity) based on appropriate predictors and to include the exposure factor in the frequency predictors. The latter is a natural choice that follows directly from the definitions of exposure, probability, and frequency factors. Indeed, it can be easily proven that frequency of design load overcoming events during $T(s)$ (i.e., $H_s$) is obtained by multiplying together the following components: 1) the rate of recurrence of the hazard event (i.e., $E_s$); 2) the likelihood that, once the hazard event occurs, the complete loading sequence will follow with the necessary timing and coincidence to result in a design load overcoming event (i.e., $P_s$). Specifically, the

frequency of overloading events is estimated as a function of the risk exposure factor and of a set of predictors mined from bridge-time-specific intermediate safety outcome factors. Similarly, the severity is evaluated by a prediction model on predictors mined from the same intermediate safety outcome factors. Finally, the risk index is obtained as shown in (3):

$$R_s \overset{\text{def}}{=} H_s(E_s, X_s) V_s(Y_s); \quad \forall s \in S \tag{3}$$

To prepare data for the frequency model, according to Step 2.2, first the frequency of $dlo \in DLO$ is defined and then computed. Specifically, it is defined as the total count of times in which the vehicular load acting on each bridge lane $i \in I$ exceeds the threshold $th_i \in TH$ defined in Step 1.5. More formally, for each $s \in S$, the frequency $H_s$ coincides with the cardinality of the $DLO(s)$. This means the count of occurrences in which a threshold is exceeded, considering all bridge lanes (4). This approach is conservative because it assumes that the lanes are independent of each other, neglecting the transverse distribution capacity of the bridge deck.

$$H_s \overset{\text{def}}{=} |DLO(s)| = \underset{i \in i; th_i \in TH}{\text{count}} (dlo \in DLO(th_i, s));$$
$$\forall s \in S \tag{4}$$

Poisson and Negative Binomial could be applied for modeling the frequency of overloading events. These may appear to be the dominant mathematical tools for modeling non-negative discrete response variables, as in the case of such events, owing to their solid statistical properties. However, exposure ($E_s$) refers to a variable for which, when equal to zero value, the frequency of events must be zero. Therefore, the prediction frequency model of load overloading can be evaluated by a Generalized Linear Model with a Negative Binomial Regression (NBR) error structure, as applied in other fields (e.g., [39], [40], [41]).

More formally, let $\alpha$, $\beta$ and $\gamma_j$ be the coefficients of the frequency model. The functional form of the frequency prediction model is as follows:

$$\widetilde{H_s} = \alpha E_s^\beta e^{\sum_{x_j \in X} \gamma_j x_{j,s}}; \quad \forall s \in S \tag{5}$$

To implement a model validation technique that relies on unbiased out-of-sample evaluation, the dataset is randomly split into training ($Tr$) and testing ($Te$) subsets.

To prepare data for the severity model, according to Step 2.3, the severity of $dlo \in DLO$ is first defined and then computed. Specifically, the severity related to $s \in S$ may be defined as the highest degree of seriousness experienced from the bridge when at least one design load overcoming event has occurred during $T(s)$. Thus, the severity can be evaluated by an ordered-response discrete variable. Because the overload associated with the ULS is a very rare event, the severity may be modeled by a binary variable (denoted with $z_s$). It takes 1 if the irreversible SLS and/or ULS thresholds are exceeded at least once in at least one $i \in I$ during $T(s)$; otherwise, it takes 0. This approach is conservative because it assumes that the lanes are independent of each other, neglecting the transverse

distribution capacity of the bridge deck. More formally:

$$z_s \overset{\text{def}}{=} \begin{cases} 1 & if \ \exists i \in i: \ (|DLO(th(FuC)_i, s)| \geq 1) \\ & or \ (|DLO(th(ChC)_i, s)| \geq 1) \\ 0 & otherwise; \end{cases}$$
$$\forall s \in S: \ H_s \neq 0; \tag{6}$$

Therefore, $V_s$ is defined as the conditional probability that $z_s$ will be equal to 1 in $s \in S$ when a non-null frequency of design load overcoming is observed (i.e., $H_s \neq 0$). More formally:

$$V_s \overset{\text{def}}{=} P(z_s = 1); \quad \forall s \in S: \ H_s \neq 0; \tag{7}$$

Because of the binary nature of the response variable, a way to build the severity prediction model is to adopt a Binomial Logistic Regression (BLR) (e.g., [39], [42]). This choice was made to facilitate the reading of the results. Indeed, they may be interpreted using the Odds Ratio (OR), which returns the number of successes (a severe event) against each failure (a non-severe event) and can be straightforward, computed by taking the exponent of the parameter estimate. More formally, let $\delta$ and $\eta_j$ be the coefficients of the severity model. The functional form of the severity prediction model is defined as follows [43]:

$$\widetilde{V_s} = P\left(z_s = 1 \underset{y_j \in Y}{|} \{y_j, s\}\right)$$
$$= \frac{e^{\delta + \sum_{y_j \in Y} \eta_j y_{j,s}}}{1 + e^{\delta + \sum_{y_j \in Y} \eta_j y_{j,s}}}; \quad \forall s \in S; \tag{8}$$

Next, according to Step 2.4, once the best frequency and severity models have been estimated, the RPM is built by joining the former with the latter. More formally:

$$\widetilde{R_s} = \widetilde{H_s} \widetilde{V_s} \tag{9}$$

The results of (9) quantitatively measure the risk for each $s \in S$, and each $s \in S$ is classified according to a risk scale to identify the most critical timeslots (STEP 2.5).

It builds on multi-level risk scales adopted in other risk analysis contexts (e.g., [39], [44]). Specifically, a five-level risk scale is proposed by establishing four thresholds to identify a range of acceptable values for all predicted $R_s$ (Table III).

Precisely, once the $\tilde{R_s}$ have been computed for each timeslot, they are organized in decreasing order. Next, four thresholds based on the $25^{th}$, $50^{th}$, $75^{th}$, and $95^{th}$ percentiles of the ordered $R_s$ distribution (denoted as $\chi_1$, $\chi_2$, $\chi_3$ and $\chi_4$, respectively)[2] are set to define the five risk levels.

---

[2]Concerning the first three thresholds (i.e., $\chi_1$, $\chi_2$ and $\chi_3$), these were chosen using a traditional statistical approach, adopting the three well-established main quartiles (i.e., $\chi_1 = Q_1 = 25^{th}$, $\chi_2 = Q_2 = 50^{th}$ and $\chi_3 = Q_3 = 75^{th}$). Regarding the fourth threshold (i.e., $\chi_4$), guidance was derived from a preliminary analysis of risk index values obtained in the real-world experiment. Specifically, it was empirically set at the $95^{th}$ percentile (i.e., $\chi_4 = 95^{th}$), because only sporadic occurrences of severe design load overcoming events were observed in timeslots with risk index values below this level. This decision aimed to strike a balance between the maximum acceptable risk and the need to avoid undue threats to bridge operability. It is worth noting that one does not have to adhere to the previous scale to use the framework, which acknowledges the freedom to establish this scale in some other ways.

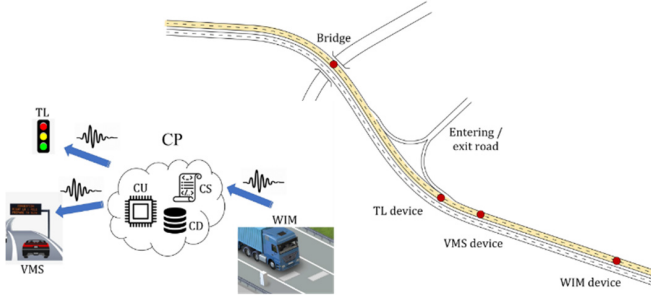| Level | Lower limit | Upper limit | Color |
|---|---|---|---|
| $RL_1$ - Maximum | $\chi_4$ | $\max R_s$ | |
| $RL_2$ - High | $\chi_3$ | $\chi_4$ | |
| $RL_3$ – Above average | $\chi_2$ | $\chi_3$ | |
| $RL_4$ – Below average | $\chi_1$ | $\chi_2$ | |
| $RL_5$ - Low | $\min R_s$ | $\chi_1$ | |



Fig. 3. Main components of the ITS-based architecture.

*3) BLOCK 3: Implement a Real-Time Risk Management Strategy:* Block 3 is organized in 4 steps. Once the risk index is computed according to (9), and critical timeslots have been highlighted, actions can be taken to address safety bridge shortcomings.

Specifically, according to Step 3.1, an ITS-based architecture to manage the traffic flowing on the bridge is implemented. As shown in *Fig. 4*, the main components of this architecture are a WIM device, a Variable Message Sign (VMS) panel, a Traffic Light (TL), and a Cloud Platform (CP). PART F (Section F.1) of the Supplementary Material section provides more details on the procedure to be used to quantitatively determine the location of physical components (WIM, VMS, TL).

The CP encompasses 1) a Cloud Database (CD) for storing WIM data; 2) a Computing Unit (CU) for processing WIM data and automatically controlling the VMS and the TL devices; and 3) a self-developed Cloud Software (CS) that integrates the required algorithms. These components reciprocally communicate through a low-latency connection (e.g., a 5G network) and are conceived to operate continuously 24 hours a day for a week.

According to Step 3.2, monitoring windows with a fixed temporal duration are defined. More formally, let $MW$ be the set of monitoring windows and $mw \in MW$ be the generic window. Each window has the same duration, denoted as $|T(mw)|$ [s]. During each $mw \in MW$, the raw traffic data are acquired by the WIM and streamed at the CD. These data are processed by the CU based on the instructions provided in the CS. Specifically, the FP and the QCA described in Step 1.2 are first executed to remove anomalies and outliers. Secondly, risk exposure and intermediate safety outcome factors are computed as described in Step 1.4. Finally, the RPM fitted

in BLOCK 2 is executed to predict the risk index associated to $mw \in MW$ (denoted as $R_{mw}$).

According to Step 3.3, traffic management actions are automatically undertaken to mitigate the risk of traffic overloading events on bridge. To perform this task, a Risk Management Algorithm (RMA) is implemented in the CS. The nature of traffic management actions is a function of the risk level predicted in every $mw \in MW$. Depending on the action's typology, the CU promptly sends a digital signal to the actuator ITS-components (i.e., the VMS and the TL) through the low-latency connection, automatically initiating the intended action.

Particularly, if $R_{mw}$ is classified as Maximum Risk Level (i.e., $RL_1$), a yellow-red cycle is triggered on the TL. Hence, access to the bridge is prevented for all vehicles in the platoon passing on the WIM during $mw \in MW$. Simultaneously, a message is displayed on the VMS. It indicates the platoon to leave the main road. Conversely, if $R_{mw}$ is classified as High-Risk Level (i.e., $RL_2$), displaying a message asking only the heaviest trucks in the platoon to leave the main road may be appropriate. Hence, this traffic control action is automatically started by the CU on the VMS. Finally, if $R_{mw}$ is classified as Above Average Risk, Below Average Risk or Low Risk levels, no risk management interventions are activated because the monitoring window is deemed to be safe enough. More formally, the RMA is described by the pseudocode in (15), in which $GVM_{lim}$ is a fixed threshold that may be chosen considering the design load associated with ChC to safeguard the bridge against ULSs and irreversible SLSs. It is important to note that the traffic management actions of RMA are intentionally kept simple to ensure practical implementation by RAs. The aim is to avoid unnecessary complications that could hinder real-world application.

---

**Algorithm 1** Risk Management

| | |
|---|---|
| 1 | **For** each $mw \in MW$ |
| 2 | **If** $(R_{mw} \in LR_1)$ **Then** |
| 3 | Display "*All vehicles must take the next exit*" on the VMS |
| 4 | **And** Trigger a yellow $-$ red cycle on the TL *(10)* |
| 5 | **Else If** $(R_{mw} \in LR_2)$ **Then** |
| 6 | Display "*All vehicles heavier than $GVM_{lim}$ must take the next exit*" on the VMS |
| 7 | **Else** Do nothing |
| 8 | **End If** |
| 9 | **End For** |

---

According to Step 3.4, the RPM and the risk scale may be periodically updated because they are built on traffic data recorded by the WIM during a fixed monitoring period. However, the traffic load hazard characteristics could change for several reasons, such as the construction of new roads (or the decommissioning of existing ones) or the development of new residential areas, commercial hubs, or industrial districts. Hence, a periodic recalibration is required to account for this variability.

## IV. REAL-WORLD EXPERIMENT

### A. Research Context

The proposed framework was experimented in Brescia (Lombardy Region, Italy), which is the second largest city in the region and one of the most important industrial and commercial hubs in Italy ( [45], [46]). The Brescia metropolitan area houses many businesses involved in processing iron and steel goods, manufacturing heavy and high-density metal products, and features several quarries extracting stone materials for construction work. Consequently, there is a substantial demand for heavy lorry transportation, which subsequently affects the road network ( [6], [7]). A bridge along Brescia's South Ring Road was selected in collaboration with the local Road Authority (RA), i.e., the Provincia of Brescia. The RA pinpointed this bridge as one facing the most significant traffic loads within its network. It is a simply supported overpass structure over a secondary road, approximately 23.50 m span length, and it is composed by 13 longitudinal precast concrete girders. In this case study, the road section has two separate carriageways, with two vehicular lanes in each direction.

### B. Results and Discussion

The overall framework was implemented in a MATLAB©️ script running on a common mobile workstation (Intel(R) Core (TM) i7-10750H CPU @ 2.60GHz 2.59 GHz processor, 32.0 GB RAM, Windows 11 Pro 64 bit).

From a general perspective, the experiments confirmed that the most time-consuming computational processes occurred within Blocks 1 and 2, taking approximately 36 minutes. This extended computation time was a result of the prolonged monitoring period considered for establishing the risk model, involving four months and around 2M raw vehicular records. In contrast, Block 3 required a computational time of about $3*10^{-3}$ s to process WIM data for the few vehicles passing through each monitoring window, generating a risk prediction. This value is negligible when compared to the duration chosen for each monitoring window (i.e., 5 s). Therefore, given the current availability of promising solutions for low-latency communication between ITS components (e.g., 5G networks [47]), risk management actions could be triggered within a timeframe compatible with an effective risk management strategy (in the order of a few milliseconds).

More specific details regarding the findings related to the three individual blocks are provided below.

*1) BLOCK 1:* A WIM device was installed by the local RA in December 2021 near the bridge on the northern carriageway. Since heavy vehicle transit is forbidden in the left lane, only the right lane was instrumented to accomplish restrictive budget limitations. Therefore, the monitored bridge lanes in this case study (i.e., $I$) comprise the right lane of the northern carriageway, identified as lane 1 (i.e., $i = 1$) in the following discussion. The adopted WIM system consists of two stainless steel plates placed on the road surface, equipped with fiber-optic sensors, connected to a data logger. It is a "10 accuracy class" instrument, according to the OIML recommendations for WIM devices [48]. Some details on WIM records acquired

TABLE IV
DETAILS OF WIM RECORDS ACQUIRED DURING
THE MONITORING PERIOD

| | |
|---|---|
| Start date | 1st January, 2022 |
| End date | 30th April, 2022 |
| Number of raw vehicular records | 2,002,320 |
| Number of anomalies detected by the FP | 1,054,821 |
| Number of outliers detected by the QCA | 42,519 |
| Number of validated vehicular records | 904,980 |

during a four-month monitoring period (i.e., $T$) are shown in Table IV.

As reported in Step 1.2, raw traffic data were pre-processed to remove anomalies and outliers by implementing the FP and QCA into the MATLAB©️ script. Although a high fraction of records was excluded (Table IV), these mainly refer to very light vehicles (i.e., cars and vans, with a GVM below 1,000 kg and an axle mass under 500 kg). The WIM device faced challenges in determining some vehicular parameters for these records. A manual check, aligning WIM records with images captured by a nearby camera, confirmed that the excluded vehicles were predominantly the lighter ones. This is because current WIM devices are primarily designed for weighing heavy vehicles rather than their lighter counterparts. Consequently, the reliability of the following analyses remains unaffected, as lighter vehicles contribute minimally to determining the traffic load on the case-study bridge, even in extreme cases (such as crowded situations).[3] Nevertheless, this outcome suggests that manufacturers should enhance the efficiency of WIM devices to attain a more comprehensive characterization of the traffic flow.

Next, the vehicular load action on the instrumented bridge lane (i.e., $G_1(t)$) was determined from the validated traffic database through the motion law analysis (Step 1.3). To achieve an adequate temporal and spatial resolution, a 0.01 s time step was chosen in the calculations. It corresponds to a maximum 0.25 m step in axle positions if the maximum speed in the validated traffic database is assumed (i.e., 90 km/h).

According to Step 1.4, $T$ was subdivided in timeslots (i.e., $s \in S$). Since the risk modeling was performed on a monthly scale, the timeslot duration was set to one hour. Thus, a total of 2,696 hourly timeslots were obtained. Next, the

---

[3]To quantitatively support this affirmation, let us consider the value of the lowest design traffic lane load threshold for the case-study bridge (i.e., 450 kN for the Frequent Combination, according to Table VII), which corresponds to a GVM of approximately 45'000 kg. Therefore, a vehicle with a GVM lower than 1,000 kg represents less than 2.2% of this threshold. Moreover, let us conservatively suppose a very short length of 2.5 m for this vehicle. Considering the span length of the case-study bridge (23.50 m) and assuming a very small distance between vehicles (0.5 m), it can easily be proven that no more than 8 of these very short vehicles can simultaneously exist on a bridge lane, even in crowded situations. These vehicles would collectively weigh no more than 8,000 kg, constituting less than 18% of the 45'000 kg design traffic lane load threshold. Hence, it is evident that the potential of these vehicles to generate even non-severe design overload events is very low. Furthermore, the negligible potential of these vehicles to generate severe design overload events is even more apparent. Indeed, the GVM of these lightweight vehicles represents no more than 1% (for one vehicle) and 7% (for 8 vehicles) of the lowest design traffic load threshold associated with a severe overloading event (i.e., 1,085 kN for the Characteristic Combination, according to Table VII).

TABLE V

GVM LIMITS PRESCRIBED BY THE ITALIAN TC FOR EACH VEHICULAR CLASS RECOGNIZED BY THE WIM SYSTEM

| Class ID | Class name | Symbolic illustration | GVM limit [kg] |
|---|---|---|---|
| 1 | Cars and vans | | 3,500 |
| 2 | Single unit trucks and buses | | 18,000 (2 axles) 25,000 (3 or more axles) |
| 3 | Articulated trucks up to 6 axles | | 30,000 (2 axles) 40,000 (4 axles) 44,000 (5 or more axles) |
| 4 | Road trains up to 6 axles | | 24,000 (3 axles) 40,000 (4 axles) 44,000 (5 or more axles) |
| 5 | More than 6-axle vehicles | | 44,000 |
| 6 | Isolated trailers | | 6,000 (one axle) 22,000 (2 axles) 26,000 (3 or more axles) |
| 7 | Unknown vehicles | ? | 44,000 |

TABLE VI

MASS LIMITS PRESCRIBED BY THE ITALIAN TC FOR SINGLE AXLES AND FOR PAIRS OF ADJACENT AXLES. FOR THE LATTER, THE MASS LIMIT IS INTENDED FOR THE WHOLE MASS ACTING ON THE PAIR

| Item | Mass limit [kg] |
|---|---|
| Single axles (interaxle greater than 2.0 m) | 12,000 |
| Adjacent axles with an interaxle lower than 1.0 m | 12,000 |
| Adjacent axles with an interaxle between 1.0 m and 1.3 m | 16'000 |
| Adjacent axles with an interaxle between 1.3 m and 2.0' m | 20'000 |

TABLE VII

DESIGN TRAFFIC LOAD THRESHOLDS: CALCULATED VALUES FOR THE INSTRUMENTED LANE OF THE CASE-STUDY BRIDGE AND THE COUNT OF OVERCOMING EVENTS DURING THE MONITORING PERIOD

| Design traffic lane load threshold | Value [kN] | Count of overcoming events during the monitoring period | Average time interval between two events (hours) |
|---|---|---|---|
| $th(FuC)_1$ | 1,464 | 0 | N/A |
| $th(ChC)_1$ | 1,085 | 14 | 204.000 |
| $th(FrC)_1$ | 450 | 15,132 | 0.189 |

intermediate safety factors were computed for each timeslot. Particularly, as for bridge-side factors, since performing an in-depth structural analysis is out of the scope of this study, only parameters related to global geometrical properties were considered. As for context factors, as the emphasis is on temporal rather than spatial risk dependence, the former were privileged. As for hazard factors, because this research is focused on traffic risk, only, those related to traffic load were considered among anthropic hazard factors. Particularly, traffic load hazard factors were grouped into traffic flow characteristics, vehicular characteristics, interaction between vehicular and bridge characteristics, compliance with TC prescriptions, and actions induced on the structure. To compute factors for compliance with TC prescriptions, Italian TC mass limits were considered for each vehicular class recognized by the WIM system (Table V) and for individual axles and axles pairs (Table VI).

Finally, the hourly flow is selected among the risk exposure factors, because it better describes the risk temporal dependence due to its greater resolution over other exposure factors, e.g., the Average Daily Traffic. PART G of the Supplementary Material section, which is self-explicative, presents the list of the risk exposure and intermediate safety factors considered in the analysis, along with corresponding descriptive statistics.

As reported in Step 1.5, the design traffic load thresholds were calculated for the instrumented lane of the case-study bridge, and the overcoming events (i.e., $dlo \in DLO$) were identified for each timeslot by applying eqn. (1). Thus, by collecting each subset $DLO(th_1, s)$, the dataset of final safety outcome factors was obtained. The results are reported in Table VII.

It also shows that, as for $th_{FuC}$, no overcoming event occurred during $T$. This is a reassuring result, since the ULS is the most adverse scenario, associated with a structural collapse or failure. Conversely, as for $th_{ChC}$, one overcoming event

every 204 hours (i.e., a return period of about 8 days) was observed. Although the ISLS is a less adverse scenario than ULS, this would seem a worrisome result since the overcoming of the associated design lane load was found to occur with a significantly greater frequency than the 1,000 years return period prescribed by the current Italian SDC (i.e., [37]). This would underscore the necessity of implementing traffic management measures on the case-study bridge to reduce the occurrence of these overloading events to comply with SDCs requirements. Notworhty a more detailed structural analysis accounting for the traffic load effect should validate this result.

Finally, as for $th_{FrC}$, 5.3 overcoming events per hour, on average, were detected. Though these events are related to the RSLS, they must be carefully assessed as they could adversely affect structural appearance, durability, or water tightness.

*2) BLOCK 2:* Once raw WIM data had been prepared, the observed frequency of overloading events was determined for each timeslot according to (4), and the frequency prediction model was built according to (5). Table VIII reports the coefficient estimates and the p-values of each factor included in the best fit model. Items in bold denote significant variables at $<.05$ level.

As a general perspective, this model fit the data well. Indeed, the statistical $\chi^2$ test on $dr$ produces a small p-value for goodness-of-fit ($< 0.001$). Additional insights into the performance of the frequency model are presented in PART H of the Supplementary Material section.

As for predictors, the results confirms that most of them are highly significant (i.e., p-value $< 0.05$), showing a strong regression effect. Focusing on each highly significant predictor separately, the following considerations result.

As for the exposure risk factor, the results show that the exponent (i.e., $\beta$) is positive, as expected (e.g., [21]).

TABLE VIII
RESULTS OF THE FREQUENCY PREDICTION MODEL

| Item | Description | Est. | p-val | Item | Description | Est. | p-val |
|---|---|---|---|---|---|---|---|
| $\log(\alpha)$ | Natural logarithm of the constant | -1.920 | 0.516 | $\gamma_8$ | Mean interaxle | 1.084 | 0.085 |
| $\beta$ | Exponent of the exposure factor | 0.400 | **<.001** | $\gamma_9$ | Maximum GVM length ratio | 0.00043 | **<.001** |
| $\gamma_1$ | Weekend (wrt weekday) | -0.510 | **<.001** | $\gamma_{10}$ | Mean GVM overload ratio – Class 1 (*Cars and vans*) | 3.910 | **0.005** |
| $\gamma_2$ | Class 2 (*Single unit trucks and buses*) fraction | -8.390 | 0.158 | $\gamma_{11}$ | Maximum GVM overload ratio – Class 2 (*Single unit trucks and buses*) | -0.151 | 0.111 |
| $\gamma_3$ | Class 5 fraction (*More than 6 axles vehicles*) | 6.950 | 0.242 | $\gamma_{12}$ | Maximum GVM overload ratio – Class 4 (*Road trains up to 6 axles*) | 0.403 | **<.001** |
| $\gamma_4$ | Mean speed | -0.042 | **<.001** | $\gamma_{13}$ | Overloaded vehicles fraction – Class 3 (*Articulated trucks up to 6 axles*) | 1.711 | **<.001** |
| $\gamma_5$ | Minimum length | -2.094 | **0.017** | $\gamma_{14}$ | Overloaded vehicles fraction – Class 4 (*Road trains up to 6 axles*) | 0.271 | **0.018** |
| $\gamma_6$ | Mean axle imbalance ratio | -1.426 | **0.011** | $\gamma_{15}$ | Extremely loaded vehicles following one another | 0.150 | **0.043** |
| $\gamma_7$ | Maximum axle imbalance ratio | 0.438 | **0.045** | $\gamma_{16}$ | Overloaded axle fraction | 19.260 | **<.001** |

**Summary statistics**

| Source | Degree of freedom | Deviance | Mean deviance | Parameter | Value |
|---|---|---|---|---|---|
| Regression | 17 | 4,303.1 | 253.13 | Deviance ratio ($dr$) | 253.13 |
| Residual | 2,139 | 569.5 | 0.266 | Global significance ($\chi^2$) | .001 |
| Total | 2,156 | 4,872.7 | 2.260 | | |

Therefore, a 1 veh/h increase in the hourly flow increases the count of overcoming events as well, while keeping all other variables constant at their means. This implies that RAs should prioritize their attention on bridges experiencing higher traffic volumes, especially during peak periods.

As for temporal context factors, the negative coefficient associated with the type of day (i.e., $\gamma_1$) indicates that the frequency was lower on the weekend. This is a consequence of the lower number of commercial activities during weekends.

As for the traffic flow characteristic factors, the speed factored significantly. Particularly, a 1 km/h increase in the mean speed reduces the count of overloading events (i.e., $\gamma_4 < 0$), while keeping all other predictors constant at their means. This result could be justified as follows. First, the faster vehicles are likelier to belong to lighter categories [6]. Second, an increase in speed reduces the permanence time on the bridge and, therefore, leads to a lower probability of multiple presences. This implies that excessively low speed limits on bridge decks could potentially compromise safety. Considering that RAs occasionally impose very low speed limits for heavy vehicles on damaged bridge decks to mitigate dynamic effects, this result is relevant and warrants further investigation [4].

As for vehicular characteristic factors, three predictors proved to be highly significant: the vehicle length, the axle imbalance ratio, and interaxle. Particularly, a 1 m increase in the minimum length reduces the count of overcoming events, while keeping all other variables constant at their means (as shown by coefficient $\gamma_5 < 0$). Maybe extending the length of shorter interposed vehicles could create separation between two successive heavy vehicles, thereby decreasing the probability of simultaneous presence on the bridge. This would imply the need for a minimum headway for heavier vehicles when passing over bridges. Conversely, as for axle imbalance factor, it has a contrasting effect, since opposite signs were found for mean and maximum axle imbalance ratios (i.e., $\gamma_6 < 0$ and $\gamma_7 > 0$).

As for the interaction between vehicular and bridge characteristic factors, the maximum mass linear density (i.e., GVM length ratio) is highly significant, and the coefficient is positive as expected (i.e., $\gamma_9 > 0$). Therefore, a 1 kg/m increase in the GVM length ratio increases the count of overcoming events while keeping all other predictors constant.

As for the compliance with TC prescriptions factors, the subgroup has the stronger influence on the frequency since six factors proved extremely significant: five related to the whole vehicle and one related to individual axles. Regarding the whole vehicle factors, the frequency increases as the GVM limit ratio and the percentage of overloaded vehicles rise (i.e., $\gamma_{10} > 0$, $\gamma_{12} > 0$, $\gamma_{13} > 0$ and $\gamma_{14} > 0$).

It indicates that vehicles exceeding TC mass limits induce a higher risk than compliant ones, which is an expected result (e.g., [8], [21]). This implies the necessity for RAs to implement additional controls to prevent violations of GVM limits for transportation carriers. Besides, a greater frequency was found when extremely loaded vehicles (GVM higher than 44'000 kg) following one another were detected (i.e., $\gamma_{15} > 0$). This endorses the findings of [21] and suggests that the queuing of extremely loaded vehicles should be prohibited on bridges. As for single axle factors, a 1% increase in the overloaded axle fraction strongly amplifies the count of overcoming events (i.e., $\gamma_{16} > 0$). It is noteworthy to report that the overloaded axle fraction emerges as the factor with the most substantial positive impact on overloading frequency. This is evident from having the greatest positive

TABLE IX
RESULTS OF THE SEVERITY PREDICTION MODEL

| Item | Description | Estim. | OR | p-val. | Item | Description | Estim. | OR | p-val. |
|------|-------------|--------|-----|--------|------|-------------|--------|-----|--------|
| $\delta$ | Constant | -188.9 | | **0.027** | $\eta_4$ | Minimum axle imbalance ratio | -38.7 | 1.56E-17 | **0.029** |
| $\eta_1$ | Maximum length | 0.464 | 1.590 | 0.061 | $\eta_5$ | Maximum GVM overload ratio | 55.8 | 1.71E+24 | **0.019** |
| $\eta_2$ | Maximum axle mass | 0.00212 | 1.002 | 0.091 | $\eta_6$ | Maximum GVM overload ratio | -23.48 | 6.35E-11 | **0.018** |
| $\eta_3$ | Mean axle imbalance | 50.4 | 7.73E+21 | 0.091 | | − Class 1 | | | |
| | ratio | | | | | (*Cars and vans*) | | | |

| Summary statistics | | | | | |
|---|---|---|---|---|---|
| Source | Degree of freedom | Deviance | Mean deviance | Parameter | Value |
| Regression | 6 | 101.02 | 16.836 | Deviance ratio ($dr$) | 16.84 |
| Residual | 1,224 | 15.16 | 0.012 | Global significance ($\chi^2$) | <.001 |
| Total | 1,230 | 116.18 | 0.094 | | |

estimate among all the coefficients. This finding aligns with expectations, given that overloaded axles contribute to adverse impacts on road infrastructures (e.g., [49]). It also confirms the need to introduce additional controls to prevent violations of axle mass limits by transportation carriers.

Next, because of Step 2.3, the observed severity of overloading events was determined (according to (6) and (7), and the severity prediction model was built (according to (8). Table IX reports the coefficient estimates and the p-values of each factor included in the best fit model. The numerical entries in bold represent significant variables at <.05 level.

From a general perspective, this model fits the data well. Indeed, the statistical $\chi^2$ test on $d.r.$ leads a small p-value for goodness-of-fit (<0.001). Further insights into the performance of the severity model are detailed in PART H of the Supplementary Material section.

As for predictors, the results confirm that many are highly significant (p-value < 0.05), showing a strong regression effect. Particularly, the highly significant factors concern vehicular characteristics (i.e., axle imbalance ratio) and compliance with TC prescriptions (i.e., maximum GVM limit ratio). Focusing on each highly significant predictor separately, the following considerations result.

As for vehicular characteristics factors, the negative coefficient of the minimum axle imbalance (i.e., $\eta_4$) (or, equivalently, OR < 1) indicates that a unit increase of minimum axle imbalance toward 1 (i.e., axle perfectly balanced) reduces the severity odds. Probably, more prudent operators are more likely to comply with mass limit prescriptions. Thus, the likelihood of observing extremely loaded vehicles on the bridge should be minor, hence decreasing the severity odds. As for the compliance with TC prescription factors, the coefficient of the maximum GVM overload ratio computed on all vehicular classes (i.e., $\eta_5$) is positive as expected (or, equivalently, OR > 1). The maximum GVM overload ratio (computed on all vehicular classes) is identified as the factor with the strongest positive impact on overload severity, according to the greatest positive coefficient's estimate.

Conversely, a negative coefficient (or, equivalently, OR < 1) was estimated for the maximum GVM overload limit ratio computed on Class 1 vehicles only (i.e., $\eta_6$). This confirms that, while heavy trucks exceeding the TC mass limits induce more severe events on the bridge than legally loaded ones,



Fig. 4. Weekly distribution of the predictions for each risk level (sunday being the first day).

an increase in the overloading ratio of light vehicles (i.e., cars and vans) does not negatively affect bridge safety.

Next, the RPM was built by joining the frequency and severity models fitted in Steps 2.2 and 2.3. Therefore, the risk index (i.e., $\tilde{R}_s$) was predicted for each $s \in S$ by applying (9), and the five-level risk scale was set up.

Some considerations emerge when the weekly and daily distribution of the predictions are explored for each risk level.

As for the weekly distribution, *Fig. 4* indicates that Wednesday (day 4) was the riskiest day due to the greatest occurrence of $RL_1$ predictions. Moreover, approximately 98.5% of maximum risk (i.e., $RL_1$) timeslots occurred from Monday (day 2) to Friday (day 6). Hence, Sunday (day 1) and Saturday (day 7) were the safest days, with the highest percentage timeslots inside $RL_4$ and $RL_5$. This is consistent with the high significance of the type-of-day factor found in the frequency model.

As for the daily distribution, *Fig. 5* shows that almost all $RL_1$ timeslots arose during daylight, with the first and the second maximum peak in the 6th and 13th hours, respectively. Since Class 5 vehicles presented their peak flow during the early morning, and permits were more likely to belong at this class,[4] permit vehicles probably had the greatest contribution in determining $RL_1$ predictions. Conversely, illegally overloaded vehicles (that more likely belong in other classes[5]) were probably the leading cause of the second maximum $RL_1$ peak. Finally, night-time turned out to be the safest period with the highest percentage of $RL_5$ timeslots. These findings

[4]This is because permits typically involve specially designed vehicles with an increased number of axles, specifically intended to carry extreme loads.

[5]This is because illegally overloaded vehicles typically involve ordinary vehicles, not specially designed with an increased number of axles.

| Hour | $RL_1$ | $RL_2$ | $RL_3$ | $RL_4$ | $RL_5$ |
|------|--------|--------|--------|--------|--------|
| 0 | 0.7% | 0.6% | 0.0% | 4.6% | 11.1% |
| 1 | 0.0% | 0.2% | 0.4% | 4.3% | 11.4% |
| 2 | 0.0% | 0.0% | 0.4% | 8.6% | 7.1% |
| 3 | 0.0% | 0.4% | 1.3% | 11.0% | 4.3% |
| 4 | 0.0% | 2.2% | 5.6% | 7.0% | 2.5% |
| 5 | 3.7% | 5.0% | 8.6% | 1.3% | 2.2% |
| 6 | 25.2% | 9.6% | 1.3% | 1.2% | 1.6% |
| 7 | 7.4% | 8.5% | 5.6% | 0.7% | 2.2% |
| 8 | 6.7% | 5.4% | 7.7% | 1.9% | 1.9% |
| 9 | 5.2% | 5.6% | 7.7% | 1.3% | 2.5% |
| 10 | 3.0% | 6.1% | 7.0% | 1.8% | 2.8% |
| 11 | 3.0% | 6.9% | 6.4% | 1.9% | 2.4% |
| 12 | 10.4% | 6.1% | 5.8% | 1.9% | 2.4% |
| 13 | 11.1% | 6.9% | 4.5% | 1.9% | 3.0% |
| 14 | 3.7% | 7.4% | 5.5% | 2.2% | 2.5% |
| 15 | 7.4% | 6.5% | 5.2% | 2.2% | 2.7% |
| 16 | 3.7% | 5.6% | 6.4% | 1.6% | 3.4% |
| 17 | 4.4% | 3.9% | 6.8% | 1.6% | 4.2% |
| 18 | 2.2% | 4.1% | 6.2% | 2.2% | 4.3% |
| 19 | 0.7% | 5.2% | 3.9% | 4.3% | 3.7% |
| 20 | 0.0% | 2.4% | 1.6% | 8.6% | 4.0% |
| 21 | 1.5% | 0.9% | 1.0% | 9.3% | 4.7% |
| 22 | 0.0% | 0.4% | 0.7% | 9.5% | 5.6% |
| 23 | 0.0% | 0.2% | 0.1% | 8.8% | 7.3% |
| Total | 100% | 100% | 100% | 100% | 100% |

Fig. 5. Daily distribution of the predictions for each risk level.

suggest that RAs should: 1) pay greater attention to the impact on bridge safety when issuing permits for extremely loaded vehicles; and 2) conduct more control activities, especially during weekday daylight hours, to identify and penalize illegally overloaded vehicles.

*3) BLOCK 3:* To manage the highest risk situations, the ITS-based architecture should be implemented as shown in Step 3.1. However, due to budget constraints, the case study is limited to a preliminary ITS architecture design and a simulation of its operativity based on real data. Hence, the location of the main physical components (i.e., WIM, VMS, and TL) was identified in a GIS environment. For more details, please refer to PART F (Section F.2) of the Supplementary Material.

As reported in Step 3.2., the procedure was simulated using a month of WIM raw data (534,729 vehicles) acquired from 1st to 31st May, 2022. Hence, 518,381 monitoring windows with a 5 s temporal duration were defined. For each monitoring window, the raw WIM data were virtually collected in actual time, streamed at the CD and pre-processed by the CU to remove anomalies and outliers according to FP e QCA algorithms. A total of 199,475 vehicles were globally preserved after the pre-processing. Next, the value of each risk explanatory factor for each monitoring window was computed by the CU, and the risk index related to each monitoring window (i.e., $R_{mw}$) was calculated instantaneously.

Traffic management actions were simulated as indicated in Step 3.3. Hence, the RMA described by the pseudocode in (10) was virtually implemented during the considered month. According to the $th(ChC)_1$ threshold, a value of 108,000 kg was set for $GVM_{lim}$ to safeguard the bridge against ULS and ISLS. Table X reports the amount of monitoring windows and vehicular flow involved in RMA actions. The number of vehicles involved in the actions is not negligible (i.e., 415).

Table XI quantifies the effectiveness of proposed traffic management actions in mitigating the risk of design load overcoming events by comparing together the following quantities:

TABLE X
AMOUNT OF MONITORING WINDOWS AND VEHICULAR FLOW INVOLVED BY RM ACTIONS

| Risk management actions | Count of involved $mw$ | Percentage of involved $mw$ | Count of involved vehicles | Percentage of involved vehicles |
|---|---|---|---|---|
| Display "All vehicles must take the next exit" on the VMS. **AND** Trigger a yellow-red cycle on the TL | 143 | 0.03 % | 196 | 0.10% |
| Display "All vehicles heavier than 108 t must take the next exit" on the VMS. | 176 | 0.03 % | 219 | 0.11% |
| Do nothing. | 518,062 | 99.94 % | 199,060 | 99.79% |

TABLE XI
QUANTIFICATION OF THE EFFECTIVENESS OF PROPOSED TRAFFIC MANAGEMENT ACTIONS IN MITIGATING THE RISK OF DESIGN LOAD OVERCOMING EVENTS DURING THE SIMULATION PERIOD

| Design traffic lane load threshold | Count of events detected during the simulation period | Count of events that would have been avoided during the simulation period | Percentage of events that would have been avoided during the simulation period |
|---|---|---|---|
| $th(FuC)_1$ | 0 | 0 | Not applicable |
| $th(ChC)_1$ | 19 | 19 | 100% |
| $th(FrC)_1$ | 5,388 | 3,364 | 62.44% |

a. The count of events detected during the simulation period for each design load threshold. This metric was obtained directly by performing the motion law analysis on actual WIM data acquired during the simulation period.

b. The count of events that would have been avoided during the simulation period if the traffic management measures were truly implemented. This metric was directly obtained by performing motion law analysis by excluding records associated with vehicles that would have been diverted before reaching the bridge.

Despite its relative simplicity, it is evident that the proposed strategy has great potential to mitigate the risk of traffic overload on the bridge. Indeed, it would have enhanced the safety of the bridge against the traffic load hazard by preventing the totality of severe overload events detected during the simulation period. Moreover, it would have also extended the lifetime of the bridge by avoiding more than 60% of non-severe overload events.[6] Finally, these findings provide empirical validation for the efficacy of the thresholds chosen to establish the five-level risk scale, upon which traffic management actions depend.

[6] The remaining (not avoided) non-severe overload events are those belonging to the lower risk levels.

## V. Conclusion

Since an extreme traffic load hazard is one of the main causes of bridge failures, realizing live risk estimation and management systems is mandatory. However, the risk induced by extreme traffic loads has rarely been explored in literature, and the existing methods required computationally expensive elaborations not compatible with a real-time risk management strategy. Indeed, while (offline) optimized bridge maintenance plans were suggested to reduce the failure risk, online traffic management procedures implemented by Intelligent Transportation System (ITS)-based architectures and driven by bridge-specific data are missing. This study contributes to the literature in a threefold manner as follows:

- Identification of a complete list of safety factors (and sub-factors) that affect design load overcoming events on bridges.
- Proposal of a framework that estimates the risk of extreme traffic load hazard and simulates its management. Specifically, this framework collects (i) WIM raw data and handles these data to provide a bridge-specific traffic load hazard dataset. Next, (ii) it specifies the risk components in terms of frequency, severity, and exposure factors. Then, it models their relationships to build a (bivariate) probabilistic Risk Prediction Model (RPM) to forecast frequency and severity components according to a set of intermediate outcome factors. Finally, (iii) it proposes an ITS-based architecture to implement live management actions.
- Illustration of the practical effectiveness of this framework in a real case-study. An easy-to-read control dashboard helps make a diagnosis of the riskiest days of the week and time slots. Moreover, a simulation is carried out of the number of times a management action should be implemented.

The proposed methodology was implemented considering 2.5M+ WIM raw data collected during a five-month period in a pilot station on a bridge along the heavy transited ring road of the city of Brescia (Italy). Both the frequency and severity components demonstrated satisfactory fitting and predictive performance. Consequently, the risk model can be considered globally effective in classifying various levels of risk. Furthermore, the overloaded axle fraction and the Gross Vehicular Mass (GVM) overload ratio emerged as the factors with the most substantial positive impacts on the frequency and severity components, respectively.

The findings have at least three main implications.

- They suggest the need for greater caution by RAs when permits for extremely overloaded vehicles are issued, since the likelihood of inducing limit states overcoming events is significantly higher than for ordinary trucks.
- They recommend enforcement strategies for the identification and sanctioning of illegally loaded vehicles traveling without any authorization.
- They highlight the need for implementing ITS-based architectures for the real-time management of the risk related to the traffic load hazard.

It is noteworthy that one might question the innovation of this work as it applies well-established EMs to forecast the frequency and severity components. However, a primary innovation of this research lies not in formulating new models but in the incorporation and utilization of existing models in an alternative setting. EMs have been widely used in various economic and engineering fields (e.g., [39], [40], [41], [43]). However, their combination into a framework for live evaluation and management of the risk posed by traffic load hazards on road bridges is a novel aspect of this study. Nevertheless, because the framework is modular, further modeling improvements could be implemented without altering other steps. Indeed, these steps are designed to operate properly despite of the mathematical form of the risk prediction models.

Besides, the generalizability of the work might be questioned given that empirical data are derived from a single bridge lane bridge in the real-world experiment. However, the significance of this research lies in the framework rather than the specific case study. The framework's validity is kept by the general formulation of its three blocks. Each step enables the use of different methods or datasets without impairing the framework's functionality. Hence, the methodology implemented is flexible and can be generalized. New input data from a different bridge makes the methodology valid to other primary roads and easily extendable to include secondary and local roads.

Moreover, someone might argue that such a refined approach to traffic management might be academic and unnecessary because a simple WIM-based threshold signaling scheme might be preferred. However, the main shortcoming of the latter strategy stems from its deterministic connotation. For example, how do you account for the probability that multiple vehicles, each with a mass below the fixed thresholds, may act simultaneously on the bridge deck and thus apply a higher load than the design one?

Finally, this study indicates new avenues for further research. First, the value of the vehicular load acting on each monitored lane was utilized in this study as a straightforward criterion to assess the frequency and severity of bridge overload as a driver of failure probability and consequences, respectively. Since it is the traffic load effect that directly influences bridge safety, an assessment of the structural response should be necessary for a specific evaluation of bridge safety. It should consider the load transversal distribution capacity of the bridge deck among the different lanes. This is because different lane load configurations can generate different demands for a given total applied lane load in terms of internal actions on structural elements. Therefore, future studies can make use of this specialized approach to better identify the limit states overcoming prompted by overloading events.

Second, although the exposure factor may even have an impact on severity, in this study it was included only in the frequency component to ensure consistency with well-accepted risk theory. Future studies could examine the effect of exposure on the severity of bridge overload, as well as develop a trivariate risk model in which the exposure factor will be considered as a response variable along with frequency and severity.

Third, EMs (i.e., Negative Binomial and Logistic Regression) were used in this research since it is easy to understand how each explanatory element affects overload risk. However, Machine Learning techniques (e.g., Artificial Neural Networks) demonstrate promising results and will be investigated as is done in other sectors of engineering (e.g., [50], [51]).

Fourth, the methodology proposed in this study partially deviates from the real-world scenario. In fact, it disregards (i) the negative effects of traffic interruptions on bridge users and on the community (e.g., increased travel times, costs, and externalities), (ii) the problem of rerouting heavy vehicles diverted from the bridge to ensure they can reach their destination via an alternative route. Future studies should integrate all these aspects, including extending the proposed methodology to the network level to prioritize traffic management actions among bridges.

Finally, the relatively low percentage of WIM records retained after pre-processing procedures suggests that WIM manufacturers should improve the efficiency of these devices to achieve a more complete characterization of the traffic flow. Specifically, reducing the minimum thresholds for measuring axle mass and total mass would enable the inclusion of lighter vehicles in a broader manner in the analysis. This adjustment would contribute to more comprehensively accounting for extreme (marginal cases) but (possible) risky situations such as crowding on the bridge.

## ACKNOWLEDGMENT

## REFERENCES

[1] M. A. Zanini, F. Faleschini, and C. Pellegrino, "Probabilistic seismic risk forecasting of aging bridge networks," *Eng. Struct.*, vol. 136, pp. 219–232, Apr. 2017, doi: 10.1016/j.engstruct.2017.01.029.

[2] G. Fiorillo and M. Ghosn, "Risk-based importance factors for bridge networks under highway traffic loads," *Struct. Infrastruct. Eng.*, vol. 15, no. 1, pp. 113–126, Jan. 2019, doi: 10.1080/15732479.2018.1496119.

[3] G. Zhang, Y. Liu, J. Liu, S. Lan, and J. Yang, "Causes and statistical characteristics of bridge failures: A review," *J. Traffic Transp. Eng.*, vol. 9, no. 3, pp. 388–406, Jun. 2022, doi: 10.1016/j.jtte.2021.12.003.

[4] R. Ventura, B. Barabino, D. Vetturi, and G. Maternini, "Bridge safety analysis based on the function of exceptional vehicle transit speed," *Open Transp. J.*, vol. 14, no. 1, pp. 222–236, Dec. 2020, doi: 10.2174/1874447802014010222.

[5] *Linee Guida Per La Classificazione e Gestione Del Rischio, la Valutazione Della Sicurezza ed il Monitoraggio Dei Ponti Esistenti*, Ministero delle Infrastrutture e dei Trasporti, Rome, Italy, 2020.

[6] R. Ventura, "Bridge's vehicular loads characterization through weigh-in-motion (WIM) systems. The case study of Brescia," *Eur. Transport/Trasporti Europei*, no. 90, pp. 1–12, Feb. 2023. [Online]. Available: https://www.istiee.unict.it/issues, doi: 10.48295/et.2023.90.6.

[7] R. Ventura, B. Barabino, D. Vetturi, and G. Maternini, "Monitoring vehicles with permits and that are illegally overweight on bridges using weigh-in-motion (WIM) devices: A case study from Brescia," *Case Stud. Transp. Policy*, vol. 13, Sep. 2023, Art. no. 101023, doi: 10.1016/j.cstp.2023.101023.

[8] G. Fiorillo and M. Ghosn, "Fragility analysis of bridges due to overweight traffic load," *Struct. Infrastruct. Eng.*, vol. 14, no. 5, pp. 619–633, May 2018, doi: 10.1080/15732479.2017.1380675.

[9] G. Fiorillo and M. Ghosn, "Procedure for statistical categorization of overweight vehicles in a WIM database," *J. Transp. Eng.*, vol. 140, no. 5, pp. 1–12, May 2014, doi: 10.1061/(asce)te.1943-5436.0000655.

[10] M. Al-Tarawneh, Y. Huang, P. Lu, and R. Bridgelall, "Weigh-in-motion system in flexible pavements using fiber Bragg grating sensors—Part A: Concept," *IEEE Trans. Intell. Transp. Syst.*, vol. 21, no. 12, pp. 5136–5147, Dec. 2020, doi: 10.1109/TITS.2019.2949242.

[11] S.-T. Jeng and L. Chu, "Tracking heavy vehicles based on weigh-in-motion and inductive loop signature technologies," *IEEE Trans. Intell. Transp. Syst.*, vol. 16, no. 2, pp. 632–641, Apr. 2015, doi: 10.1109/TITS.2014.2333003.

[12] E. A. Micu et al., "Evaluation of the extreme traffic load effects on the forth road bridge using image analysis of traffic data," *Adv. Eng. Softw.*, vol. 137, Nov. 2019, Art. no. 102711, doi: 10.1016/j.advengsoft.2019.102711.

[13] C. Li et al., "Seismic performance assessment of a sea-crossing cable-stayed bridge system considering soil spatial variability," *Rel. Eng. Syst. Saf.*, vol. 235, Jul. 2023, Art. no. 109210, doi: 10.1016/j.ress.2023.109210.

[14] S. A. Argyroudis and S. A. Mitoulis, "Vulnerability of bridges to individual and multiple hazards-floods and earthquakes," *Rel. Eng. Syst. Saf.*, vol. 210, Jun. 2021, Art. no. 107564, doi: 10.1016/j.ress.2021.107564.

[15] S. Thöns and M. G. Stewart, "On decision optimality of terrorism risk mitigation measures for iconic bridges," *Rel. Eng. Syst. Saf.*, vol. 188, pp. 574–583, Aug. 2019, doi: 10.1016/j.ress.2019.03.049.

[16] D. Proske and M. Curbach, "Risk to historical bridges due to ship impact on German inland waterways," *Rel. Eng. Syst. Saf.*, vol. 90, nos. 2–3, pp. 261–270, Nov. 2005, doi: 10.1016/j.ress.2004.10.003.

[17] G. Fiorillo and H. Nassif, "Development of a risk assessment module for bridge management systems in New Jersey," *Transp. Res. Rec., J. Transp. Res. Board*, vol. 2674, no. 9, pp. 324–337, Sep. 2020, doi: 10.1177/0361198120929016.

[18] B. Zhu and D. M. Frangopol, "Time-variant risk assessment of bridges with partially and fully closed lanes due to traffic loading and scour," *J. Bridge Eng.*, vol. 21, no. 6, pp. 1–15, Jun. 2016, doi: 10.1061/(asce)be.1943-5592.0000817.

[19] A. Decò and D. M. Frangopol, "Life-cycle risk assessment of spatially distributed aging bridges under seismic and traffic hazards," *Earthq. Spectra*, vol. 29, no. 1, pp. 127–153, Feb. 2013, doi: 10.1193/1.4000094.

[20] A. Decò and D. M. Frangopol, "Risk assessment of highway bridges under multiple hazards," *J. Risk Res.*, vol. 14, no. 9, pp. 1057–1089, Oct. 2011, doi: 10.1080/13669877.2011.571789.

[21] G. Fiorillo and M. Ghosn, "Risk-based life-cycle analysis of highway bridge networks under budget constraints," *Struct. Infrastruct. Eng.*, vol. 18, nos. 10–11, pp. 1457–1471, Nov. 2022, doi: 10.1080/15732479.2022.2059525.

[22] A. Abarca, R. Monteiro, and G. J. O'Reilly, "Simplified methodology for indirect loss-based prioritization in roadway bridge network risk assessment," *Int. J. Disaster Risk Reduction*, vol. 74, May 2022, Art. no. 102948, doi: 10.1016/j.ijdrr.2022.102948.

[23] S. M. Wong, C. J. Onof, and R. E. Hobbs, "Models for evaluating the costs of bridge failure," *Proc. Inst. Civil Eng.-Bridge Eng.*, vol. 158, no. 3, pp. 117–128, Sep. 2005, doi: 10.1680/bren.2005.158.3.117.

[24] D. Y. Yang and D. M. Frangopol, "Life-cycle management of deteriorating bridge networks with network-level risk bounds and system reliability analysis," *Struct. Saf.*, vol. 83, Mar. 2020, Art. no. 101911, doi: 10.1016/j.strusafe.2019.101911.

[25] E. Cosenza and D. Losanno, "Assessment of existing reinforced-concrete bridges under road-traffic loads according to the New Italian guidelines," *Struct. Concrete*, vol. 22, no. 5, pp. 2868–2881, Oct. 2021, doi: 10.1002/suco.202100147.

[26] U. A. Wijesuriya and A. G. Tennant, "Binary logistic regression approach for decision making in bridge management," *Infrastruct. Asset Manag.*, vol. 9, no. 2, pp. 89–99, Jun. 2022, doi: 10.1680/jinam.21.00011.

[27] C. Davis-McDaniel, M. Chowdhury, W. Pang, and K. Dey, "Fault-tree model for risk assessment of bridge failure: Case study for segmental box girder bridges," *J. Infrastruct. Syst.*, vol. 19, no. 3, pp. 326–334, Sep. 2013, doi: 10.1061/(asce)is.1943-555x.0000129.

[28] S. Sabatino, D. M. Frangopol, and Y. Dong, "Sustainability-informed maintenance optimization of highway bridges considering multi-attribute utility and risk attitude," *Eng. Struct.*, vol. 102, pp. 310–321, Nov. 2015, doi: 10.1016/j.engstruct.2015.07.030.

[29] B. Adey, R. Hajdin, and E. Brühwiler, "Risk-based approach to the determination of optimal interventions for bridges affected by multiple hazards," *Eng. Struct.*, vol. 25, no. 7, pp. 903–912, Jun. 2003, doi: 10.1016/s0141-0296(03)00024-5.

[30] D. Dan, Y. Ying, and L. Ge, "Digital twin system of bridges group based on machine vision fusion monitoring of bridge traffic load," *IEEE Trans. Intell. Transp. Syst.*, vol. 23, no. 11, pp. 22190–22205, Nov. 2022, doi: 10.1109/TITS.2021.3130025.

[31] D. Y. Yang and D. M. Frangopol, "Risk-informed bridge ranking at project and network levels," *J. Infrastruct. Syst.*, vol. 24, no. 3, Sep. 2018, Art. no. 04018018, doi: 10.1061/(asce)is.1943-555x.0000430.

[32] D. Saydam, P. Bocchini, and D. M. Frangopol, "Time-dependent risk associated with deterioration of highway bridge networks," *Eng. Struct.*, vol. 54, pp. 221–233, Sep. 2013, doi: 10.1016/j.engstruct.2013.04.009.

[33] I. R. Parekh, D. R. Graber, and R. H. Berger, "Comprehensive bridge posting policy," *Trans. Res. Rec.*, vol. 1083, pp. 35–45, 1986.

[34] B. Zhu and D. M. Frangopol, "Risk-based approach for optimum maintenance of bridges under traffic and earthquake loads," *J. Struct. Eng.*, vol. 139, no. 3, pp. 422–434, Mar. 2013, doi: 10.1061/(asce)st.1943-541x.0000671.

[35] *Road Traffic Safety (RTS) Management Systems: Requirements With Guidance for Use*, Standard ISO 39001, Geneva, Switzerland, 2012.

[36] *Eurocode 1: Actions on Structures—Part 2: Traffic Loads on Bridges*, Eur. Union, Bruxelles, Belgium, 2003.

[37] *Norme Tecniche Per Le Costruzioni*, IMI and NTC, Gazzetta Ufficiale Della Repubblica Italiana, Rome, Italy, 2018.

[38] W. T. Fine, "Mathematical evaluation for controlling hazards," *J. Saf. Res*, vol. 3, pp. 157–166, Jan. 1971.

[39] B. Barabino, M. Bonera, G. Maternini, A. Olivo, and F. Porcu, "Bus crash risk evaluation: An adjusted framework and its application in a real network," *Accident Anal. Prevention*, vol. 159, Sep. 2021, Art. no. 106258, doi: 10.1016/j.aap.2021.106258.

[40] H. Liu, R. A. Davidson, D. V. Rosowsky, and J. R. Stedinger, "Negative binomial regression of electric power outages in hurricanes," *J. Infrastruct. Syst.*, vol. 11, no. 4, pp. 258–267, Dec. 2005, doi: 10.1061/(asce)1076-0342(2005)11:4(258).

[41] B. Barabino, M. Di Francesco, and R. Ventura, "Evaluating fare evasion risk in bus transit networks," *Transp. Res. Interdiscipl. Perspect.*, vol. 20, Jul. 2023, Art. no. 100854, doi: 10.1016/j.trip.2023.100854.

[42] S. Kameshwar and J. E. Padgett, "Multi-hazard risk assessment of highway bridges subjected to earthquake and hurricane hazards," *Eng. Struct.*, vol. 78, pp. 154–166, Nov. 2014, doi: 10.1016/j.engstruct.2014.05.016.

[43] W. H. Greene, *Econometric Analysis*, Upper Saddle River, NJ, USA: Pearson Education, 2003.

[44] U. Barua and R. Tay, "Severity of urban transit bus crashes in Bangladesh," *J. Adv. Transp.*, vol. 44, no. 1, pp. 34–41, Jan. 2010, doi: 10.1002/atr.104.

[45] V. Martinelli, R. Ventura, M. Bonera, B. Barabino, and G. Maternini, "Effects of urban road environment on vehicular speed. Evidence from Brescia (Italy)," *Transp. Res. Proc.*, vol. 60, pp. 592–599, Jan. 2022, doi: 10.1016/j.trpro.2021.12.076.

[46] V. Martinelli, R. Ventura, M. Bonera, B. Barabino, and G. Maternini, "Estimating operating speed for county road segments—Evidence from Italy," *Int. J. Transp. Sci. Technol.*, vol. 12, no. 2, pp. 560–577, Jun. 2023, doi: 10.1016/j.ijtst.2022.05.007.

[47] D. Rico and P. Merino, "A survey of end-to-end solutions for reliable low-latency communications in 5G networks," *IEEE Access*, vol. 8, pp. 192808–192834, 2020, doi: 10.1109/ACCESS.2020.3032726.

[48] *Automatic Instruments for Weighing Road Vehicles in Motion and Measuring Axle Loads Part 1: Metrological and Technical Requirements—Tests*, Standard OIML R 134-1, 2006.

[49] J. Zhao, H. Wang, and P. Lu, "Impact analysis of traffic loading on pavement performance using support vector regression model," *Int. J. Pavement Eng.*, vol. 23, no. 11, pp. 3716–3728, Sep. 2022, doi: 10.1080/10298436.2021.1915493.

[50] R. Ventura, A. Ghirardi, D. Vetturi, G. Maternini, and B. Barabino, "Comparing the vibrational behaviour of e-kick scooters and e-bikes: Evidence from Italy," *Int. J. Transp. Sci. Technol.*, Nov. 2023, doi: 10.1016/j.ijtst.2023.10.010.

[51] Z. Xu and J. H. Saleh, "Machine learning for reliability engineering and safety applications: Review of current status and future opportunities," *Rel. Eng. Syst. Saf.*, vol. 211, Jul. 2021, Art. no. 107530, doi: 10.1016/j.ress.2021.107530.

**Roberto Ventura** received the master's degree in civil engineering in 2019 and the Ph.D. degree in civil and environmental engineering, international cooperation and mathematics (curriculum of urban planning and mobility) from the University of Brescia, Italy, in 2023. He is currently a Post-Doctoral Researcher with the University of Brescia. His primary research interests include the safety of the infrastructures subjected to heavy vehicle transit, risk analyses on transportation field, and micromobility vehicles.
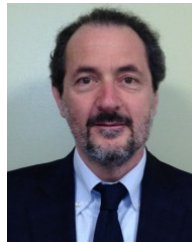
**Giulio Maternini** has been a Rector's Deputy as the Mobility Manager of the University of Brescia, Italy, since 2004. From 2010 to 2014, he was the Italian President of Italian Association of Traffic and Transportation (AIIT). Since 2012, he has been a Remote Referee with Italian Ministry of University and Research (MIUR) funding calls. Since 2019, he has been the Director of the Friendly City Study Center (CeSCAM). He is currently a Full Professor in transportation engineering with the University of Brescia. His research interests include transport infrastructures, road design, and safety in transport. Since 2018, he has been an Editor of *European Transport*.

**Benedetto Barabino** received the Ph.D. degree in transportation technology and economics from the University of Palermo in 2007. From 2019 to 2022, he was an Assistant Professor (tenure track) in transportation engineering with the University of Brescia. From 2017 to 2019, he was the Head of the Department of Study and Research, CTM, Cagliari, Italy. From 2010 to 2016, he was the Managing Director of Technomobility Ltd., a research society in the public transport industry. He is currently an Associate Professor in transportation engineering with the University of Brescia, Italy. His research interests include intelligent transportation systems, public transport planning, operations, service quality, bus safety, and fare evasion. In 2023, he was included in World's 2% Top Scientists—Elsevier BV, Stanford University, USA.